Electronic Supplementary Material (ESI) for CrystEngComm.


# Crystallographic studies of 2-picolyl substituted naphthalene diimide and bis-phthalimide ligands and their supramolecular coordination chemistry

*June I. Lovitt,[a] Chris S. Hawes,[b]*and Thorfinnur Gunnlaugsson[a*]*

[a] School of Chemistry and Trinity Biomedical Science Institute, University of Dublin, Trinity College Dublin, Dublin 2 (Ireland)

[b] School of Chemical and Physical Sciences, Keele University, Keele ST5 5BG, United Kingdom

**Supporting Information**

1. **X-Ray Powder Diffraction Patterns** **2**
2. **Thermogravimetric Analysis** **7**
3. **Spectroscopic Data** **11**
4. **NMR Spectra** **12**
5. **Hydrogen Bonding Parameters, Additional Crystallographic Figures, and Ellipsoid Plots** **14**

## 1. X-Ray Powder Diffraction Patterns

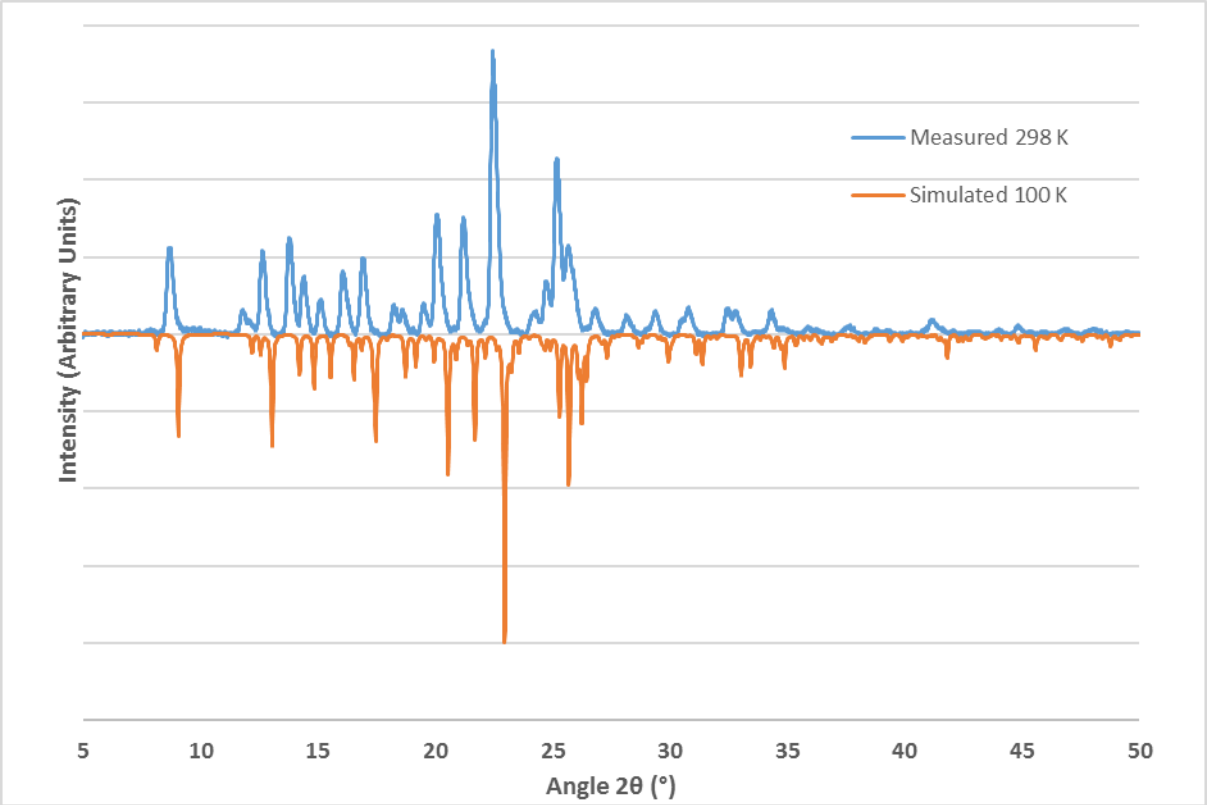


**Figure S1**: X-ray powder diffraction pattern for **L2** collected at 298 K compared to the calculated pattern from the single crystal dataset at 100 K.

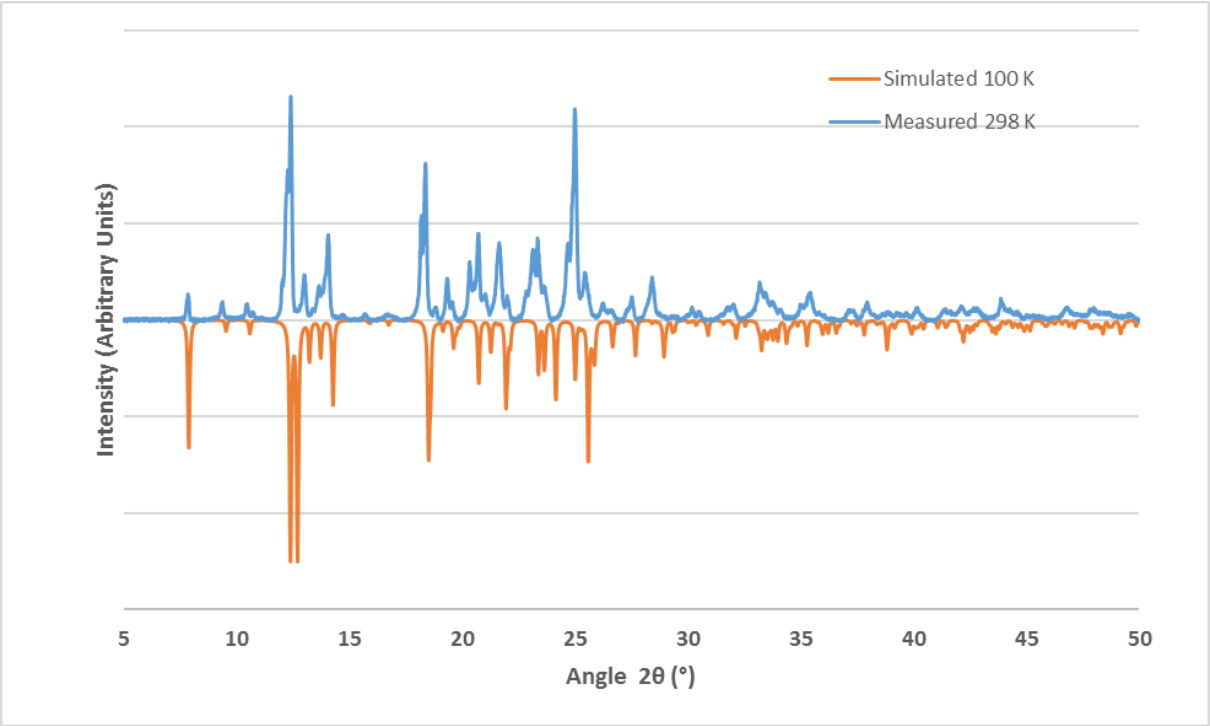


**Figure S2**: X-ray powder diffraction pattern for compound **1** at 298 K compared to the calculated pattern from the single crystal dataset (100 K).

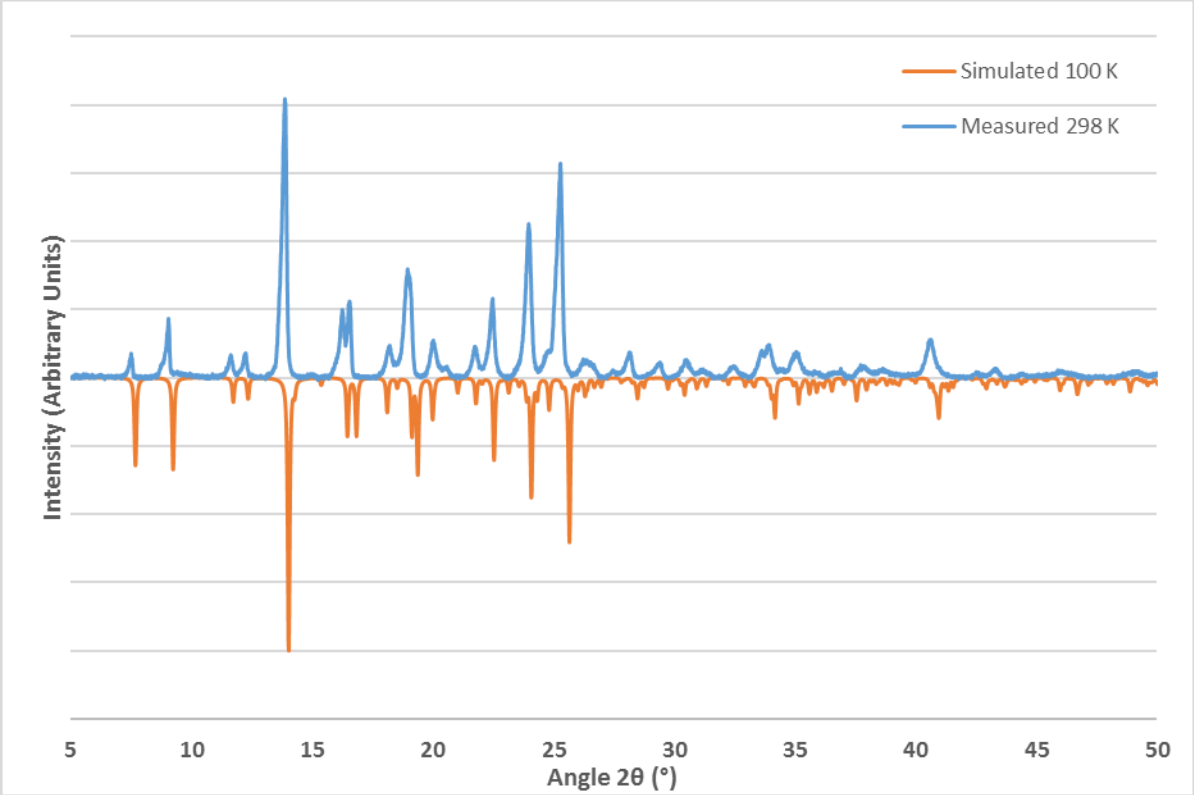


**Figure S3**: X-ray powder diffraction pattern for compound **2** at 298 K compared to the calculated pattern from the single crystal dataset at 100 K.

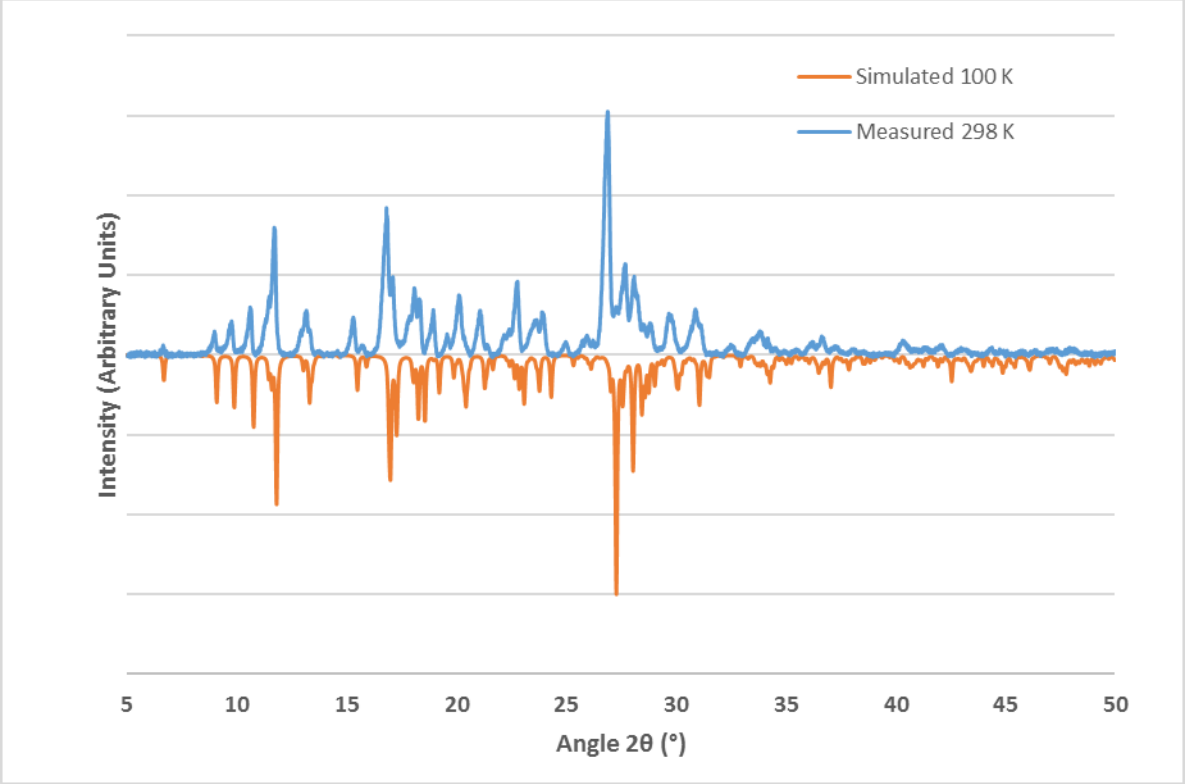


**Figure S4**: X-ray powder diffraction for compound **3** at 298 K compared to the calculated pattern from the single crystal dataset 100 K.

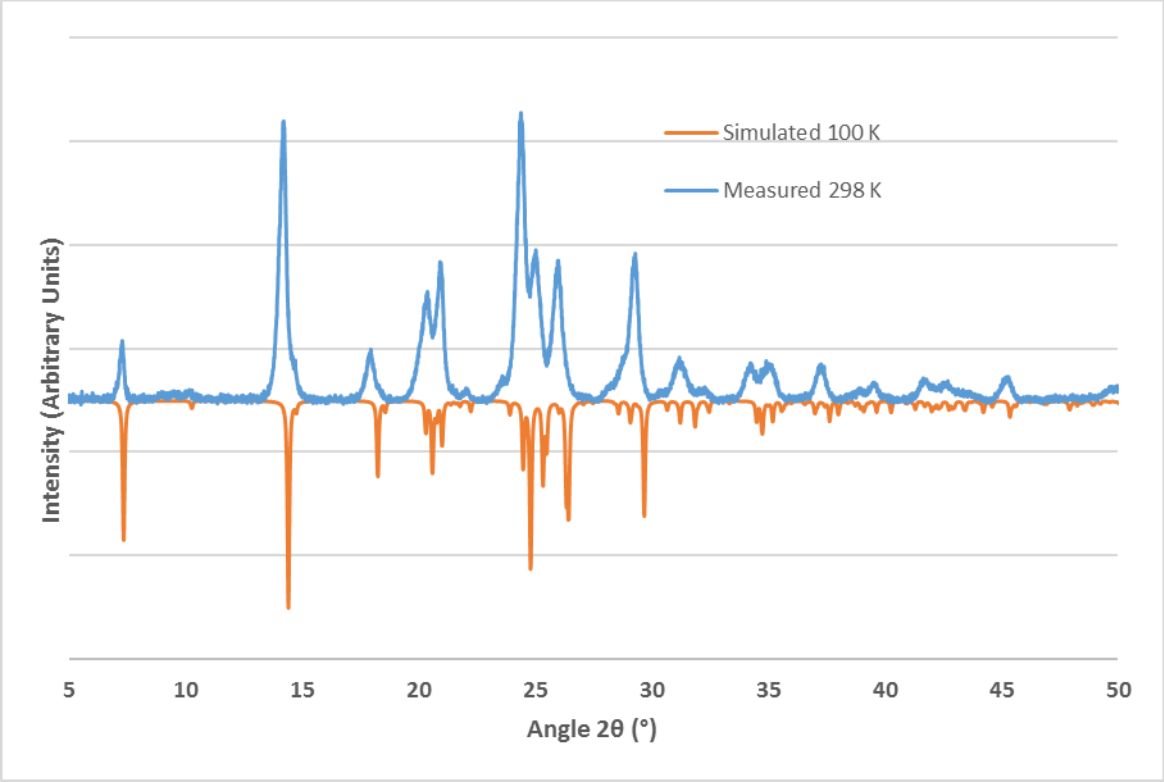


**Figure S5**: X-ray powder diffraction pattern for compound **4** at 298 K compared to the calculated pattern from the single crystal dataset at 100 K.

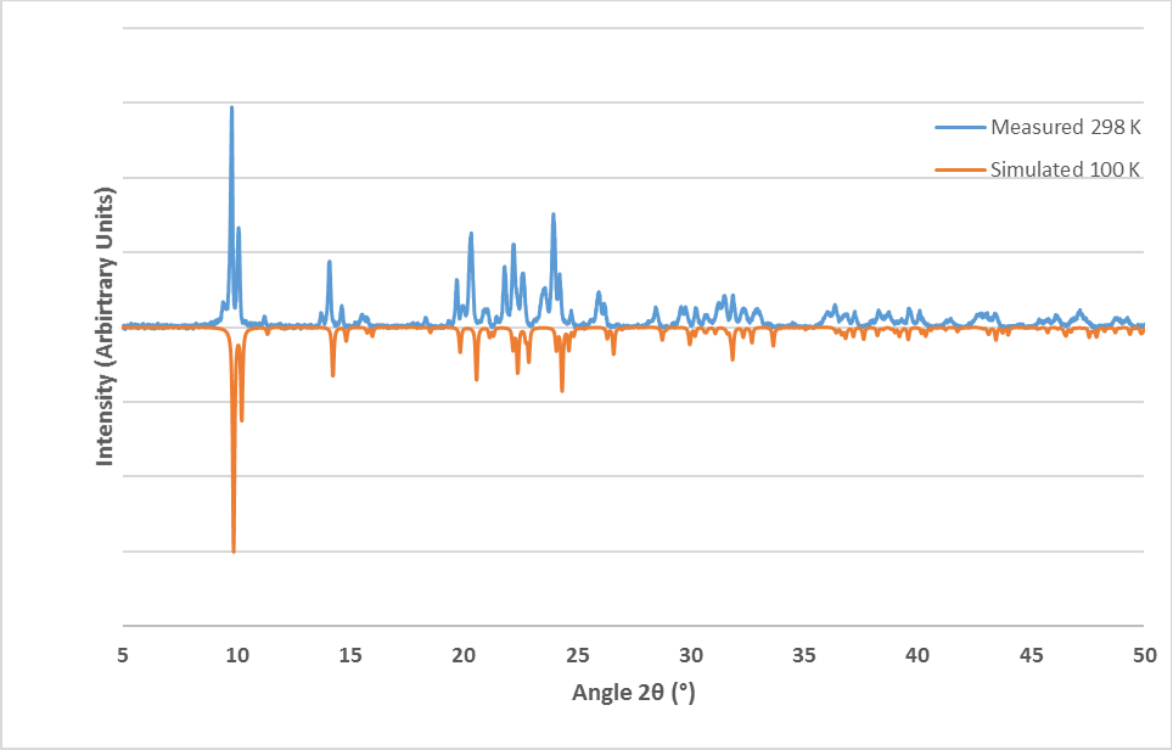


**Figure S6**: X-ray powder diffraction pattern for compound **5** at 298 K compared to the calculated pattern from the single crystal dataset at 100 K.

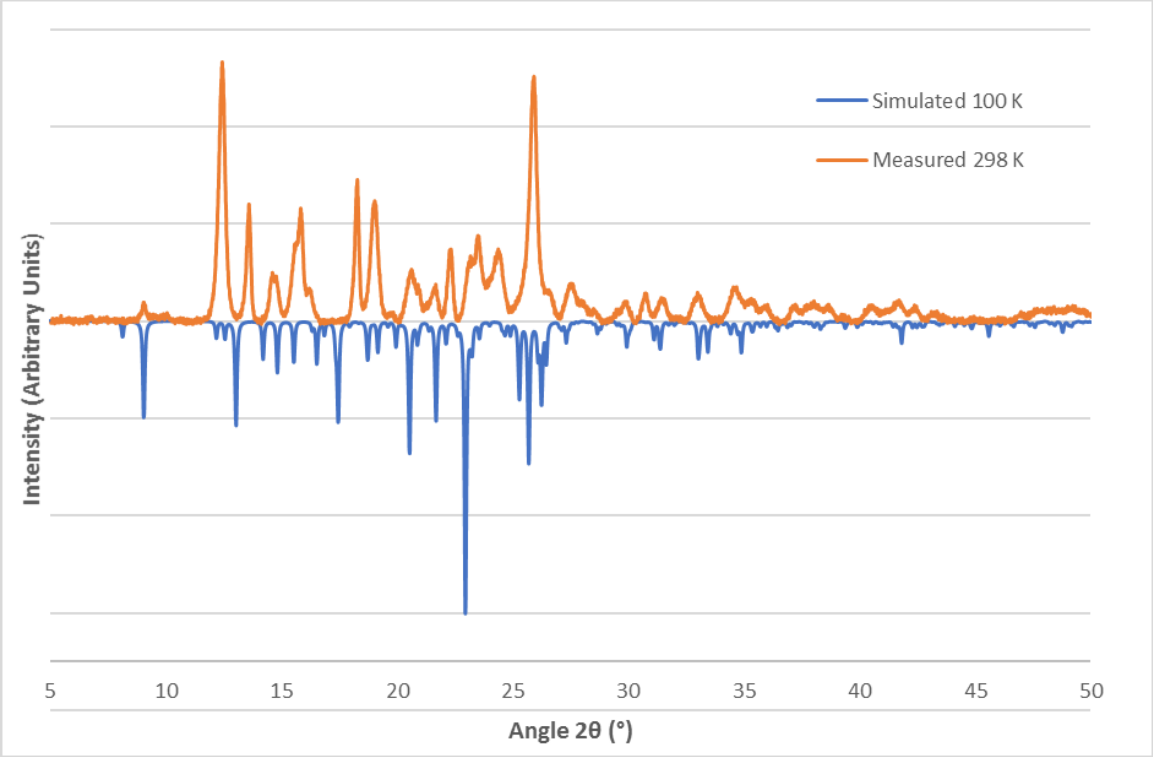


**Figure S7**: X-ray powder diffraction pattern for **L2** under analogous conditions to compound **1** formation at 298 K compared to the calculated pattern from the single crystal dataset of **L2** at 100 K.

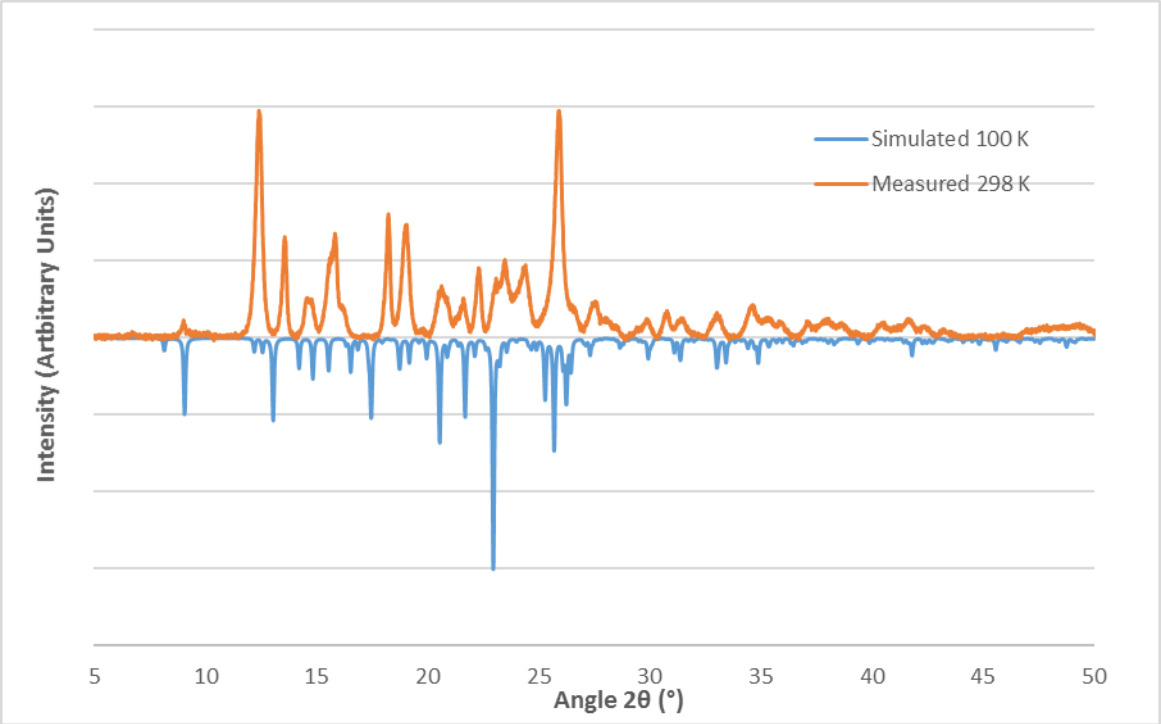


**Figure S8**: X-ray powder diffraction pattern for **L2** under analogous conditions to compound **2** formation at 298 K compared to the calculated pattern from the single crystal dataset of **L2** at 100 K.

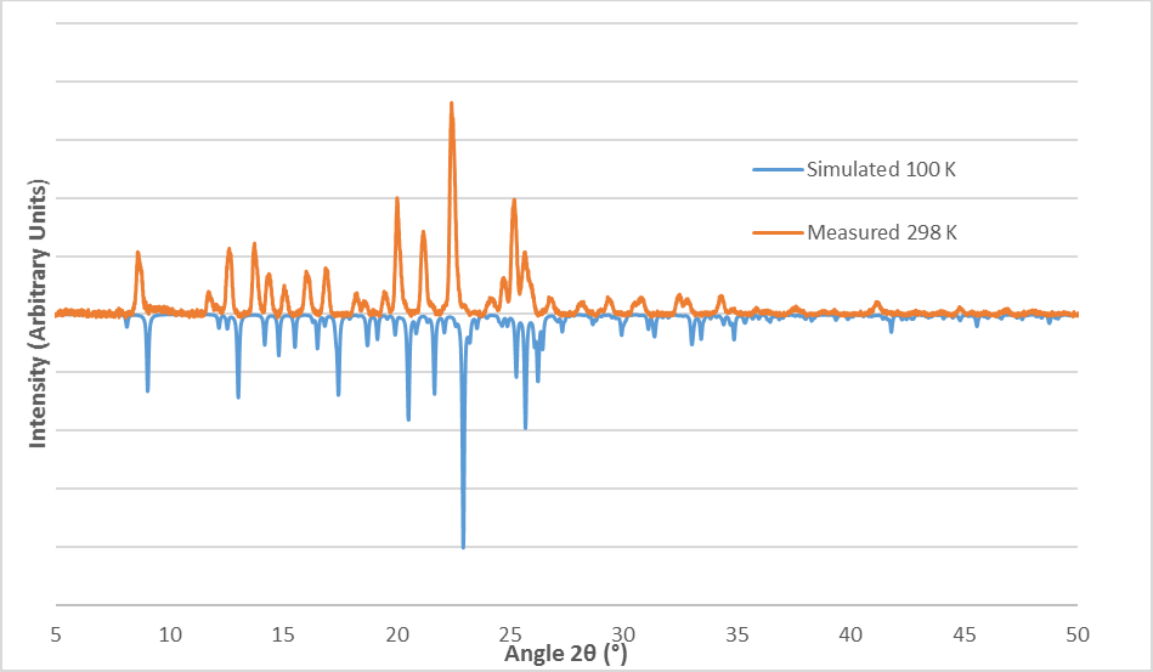


**Figure S9**: X-ray powder diffraction pattern for **L2** under analogous conditions to compound **3** formation at 298 K compared to the calculated pattern from the single crystal dataset of **L2** at 100 K.

## 2. Thermogravimetric Analysis

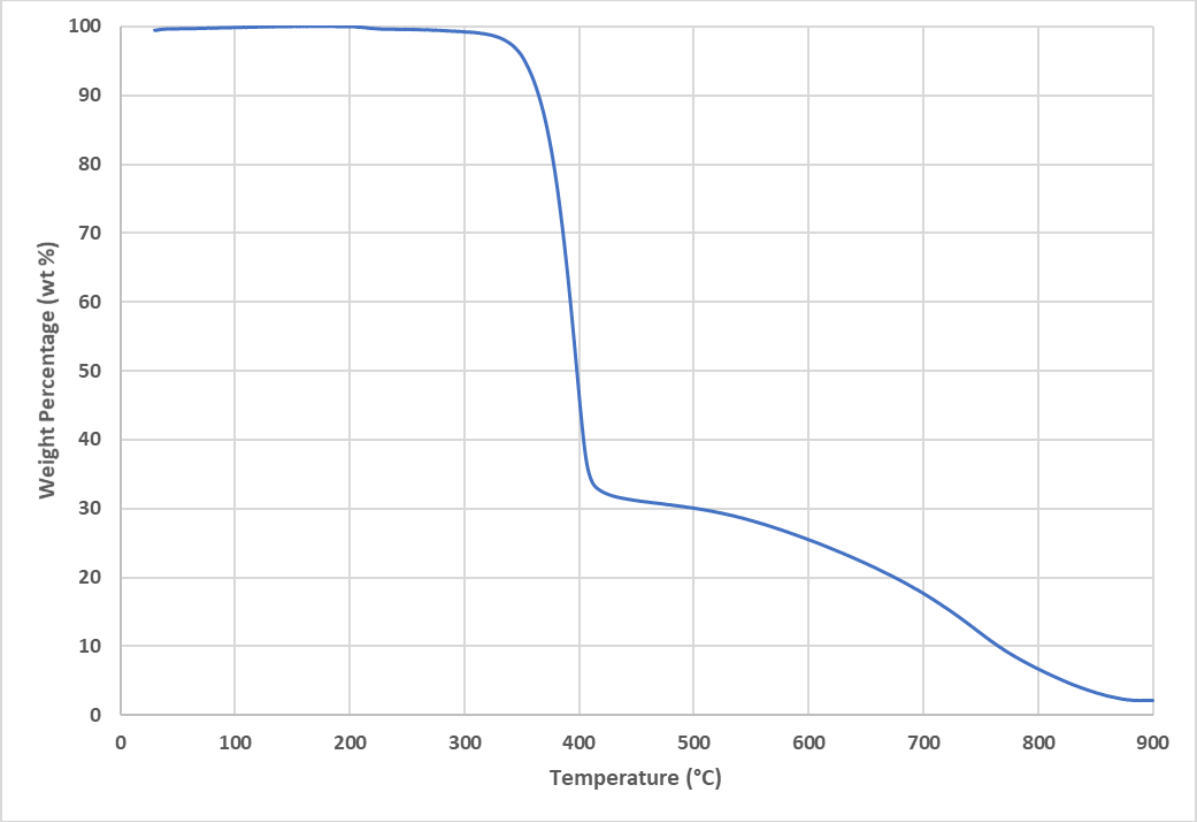


**Figure S10**: Thermogravimetric analysis for **L1.**

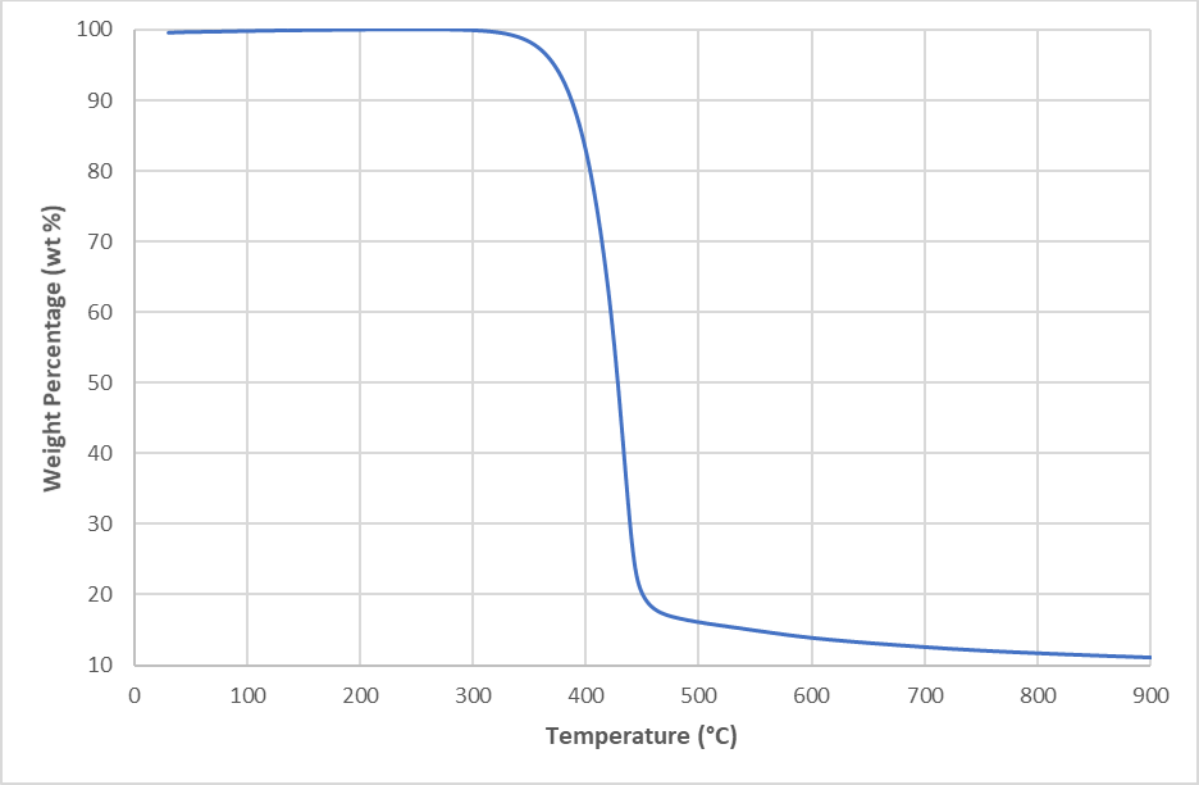


**Figure S11**: Thermogravimetric analysis for **L2.**

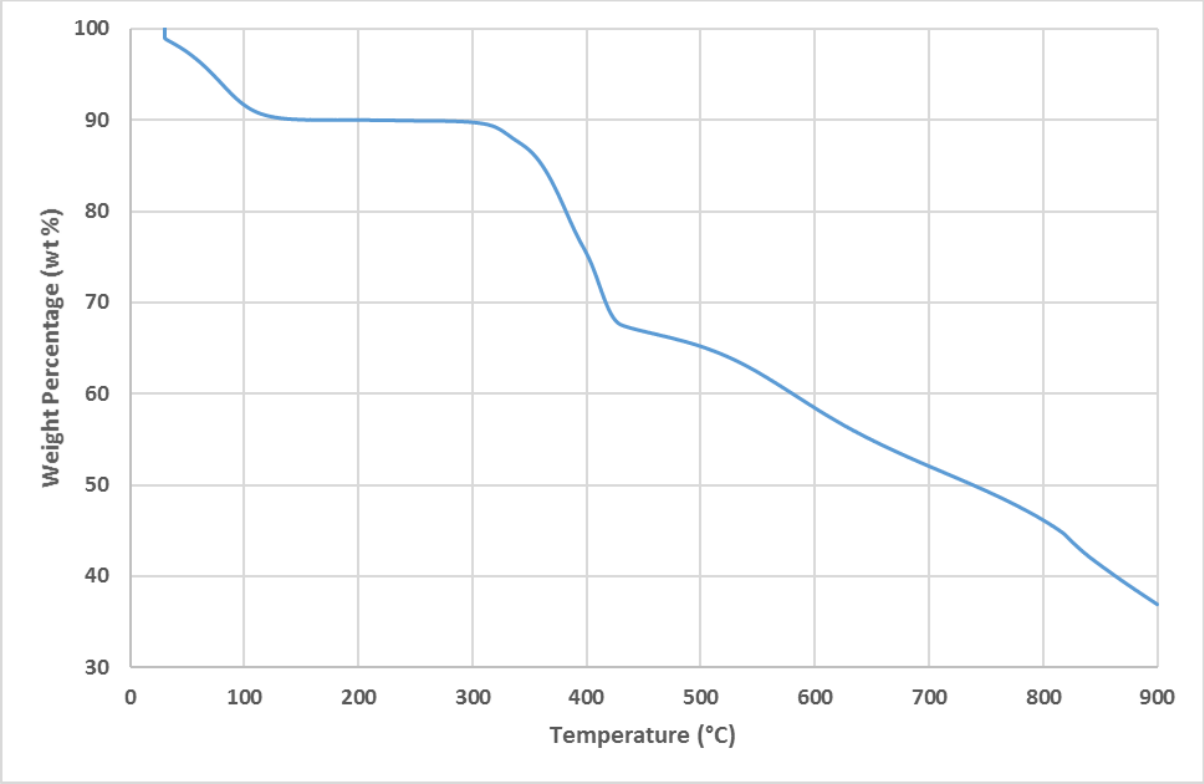


**Figure S12**: Thermogravimetric analysis for compound **1.**

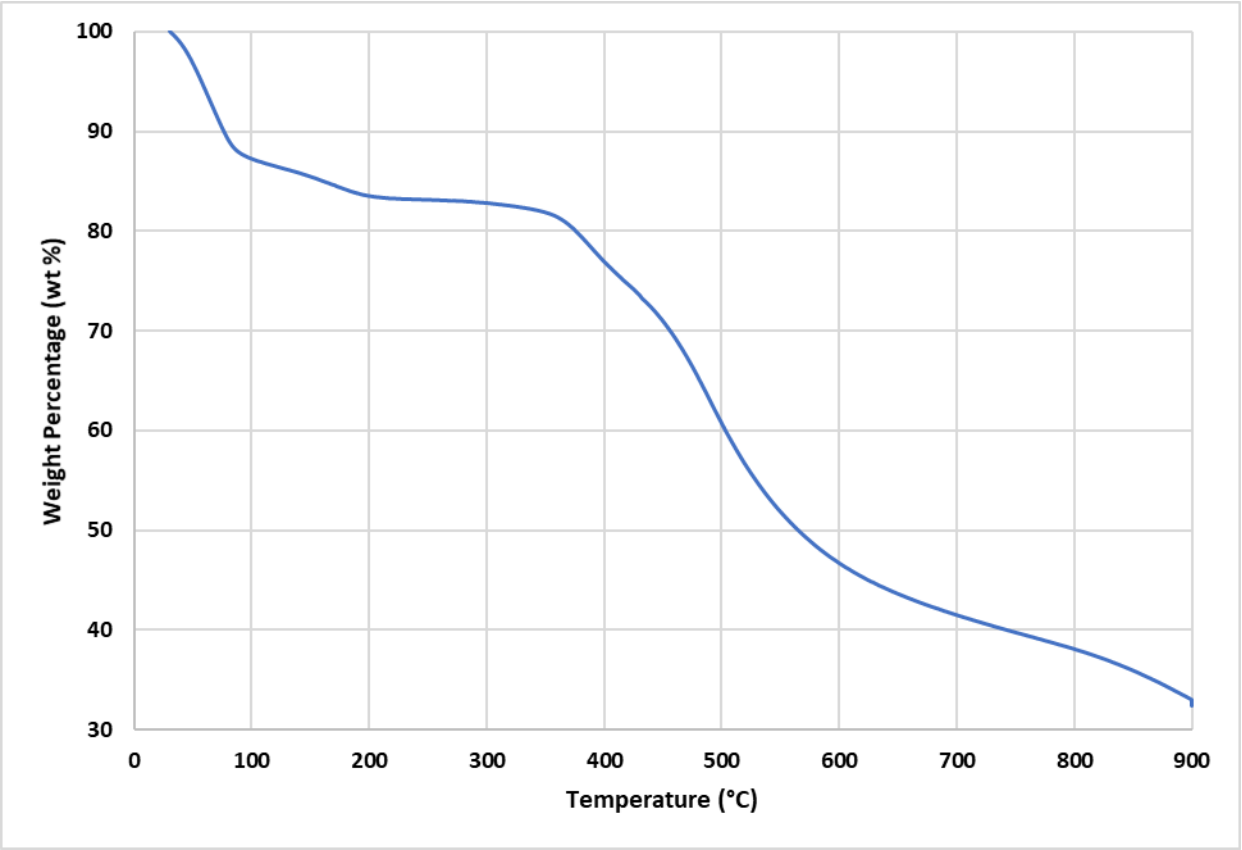


**Figure S13**: Thermogravimetric analysis for compound **1** after desolvation and rehydration in air**.**

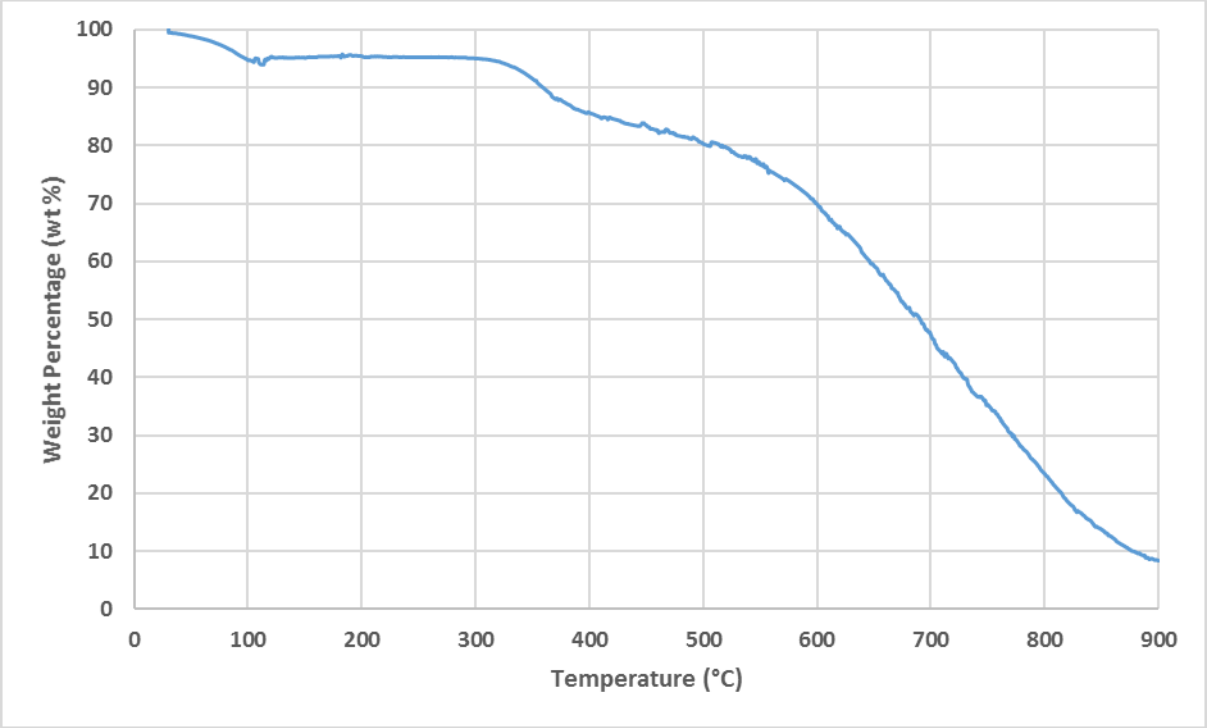


**Figure S14**: Thermogravimetric analysis for compound **2.**

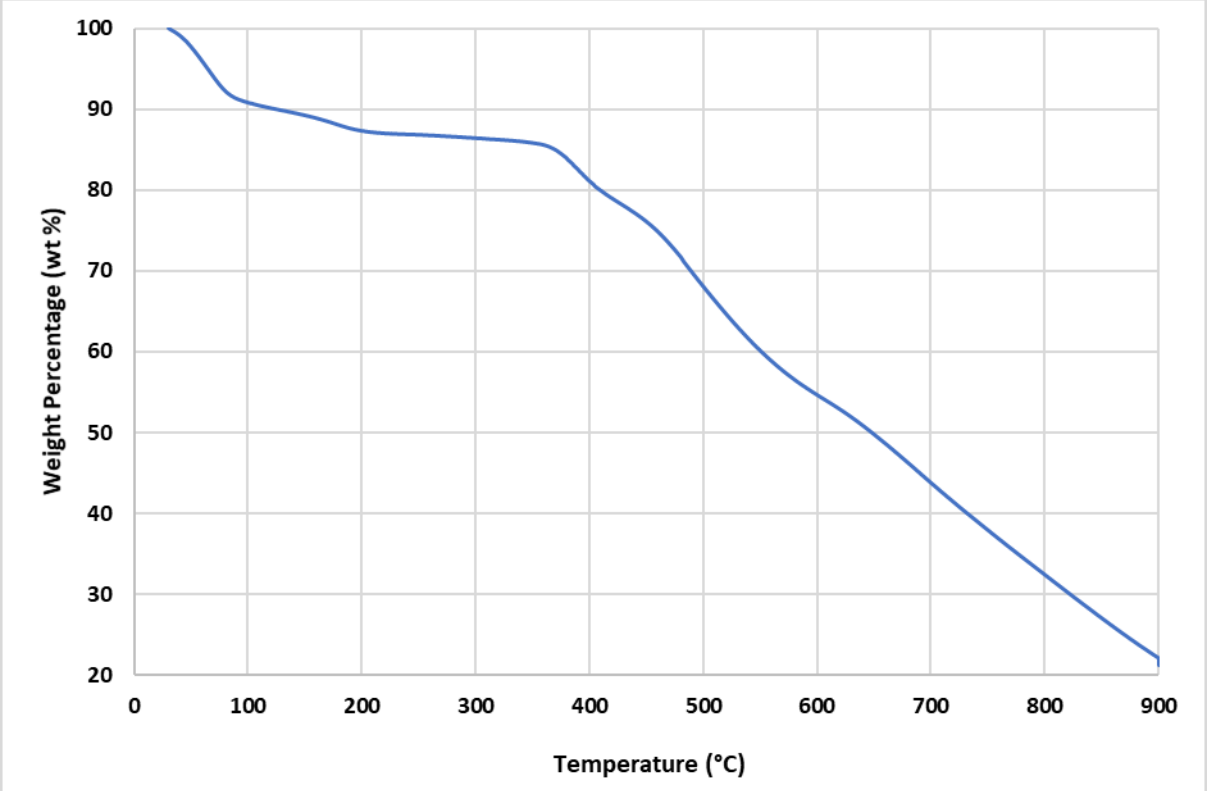


**Figure S15**: Thermogravimetric analysis for compound **2** after desolvation and rehydration in air**.**

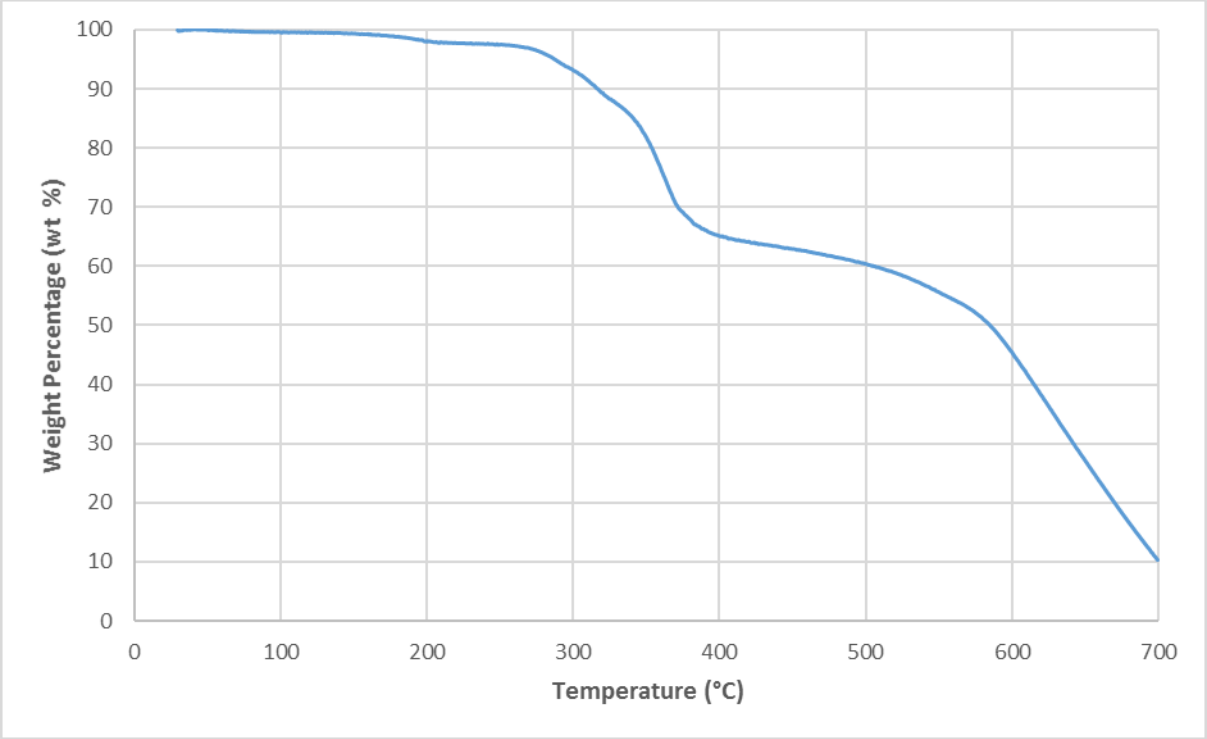


**Figure S16**: Thermogravimetric analysis for compound **3.**

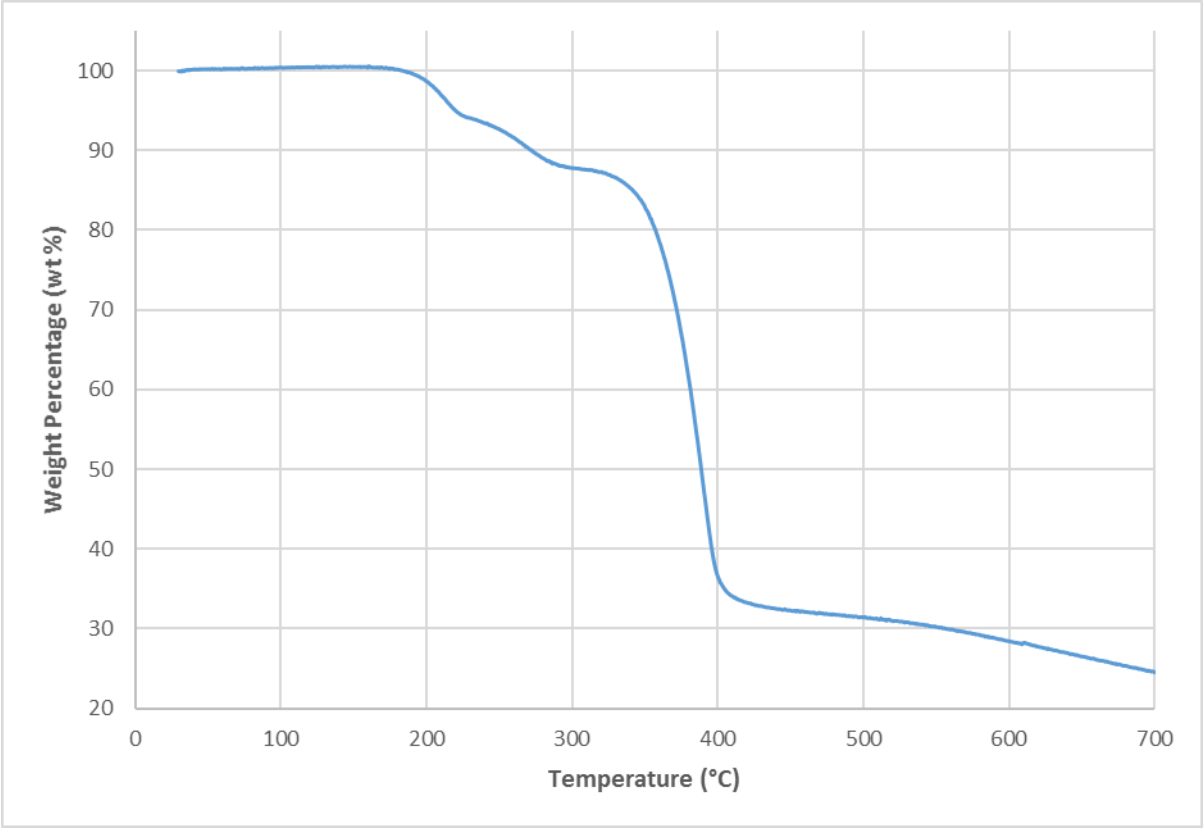


**Figure S17:** Thermogravimetric analysis for compound **4**.

## 3. Spectroscopic Data

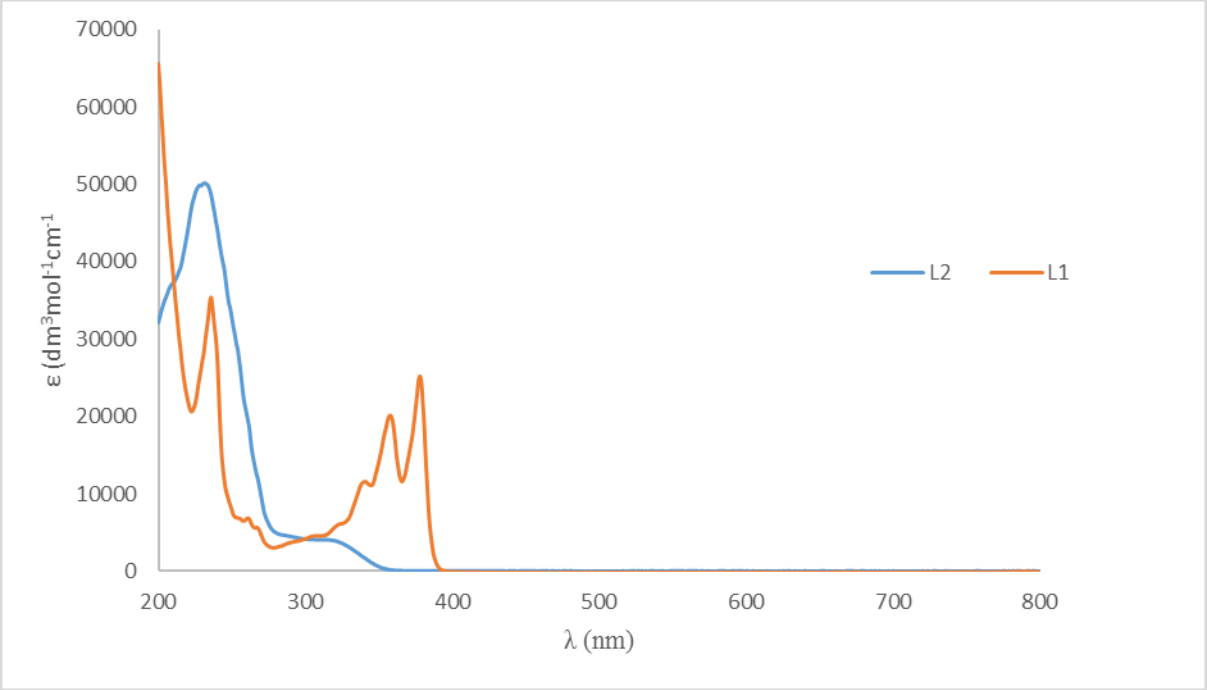


**Figure S18:** UV absorption spectra of **L1** and **L2** (MeCN) at $2x10^{-5}$M concentration.

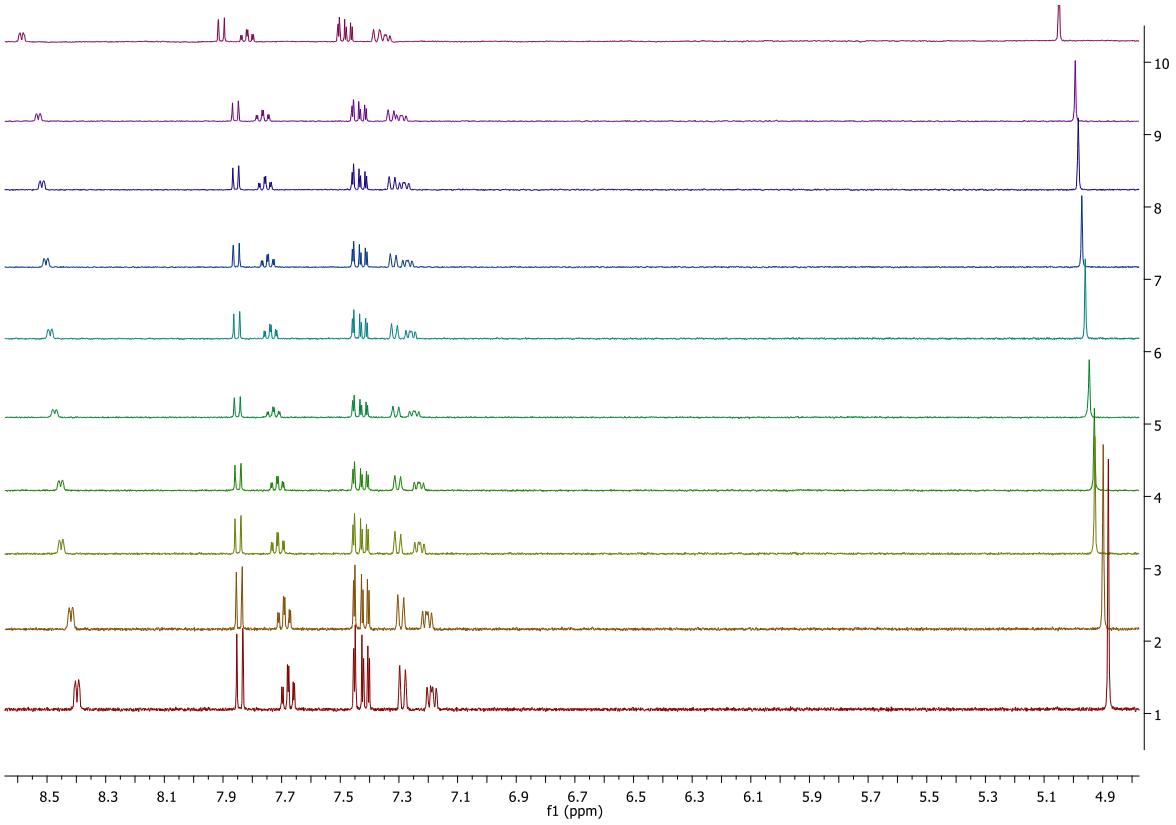


**Figure S19**: $^1$H NMR titration ($d_3$-MeCN) of the addition of $ZnCl_2$ to **L2**. Each addition represents 0.2 equivalents of $ZnCl_2$.

## 4. NMR Spectra

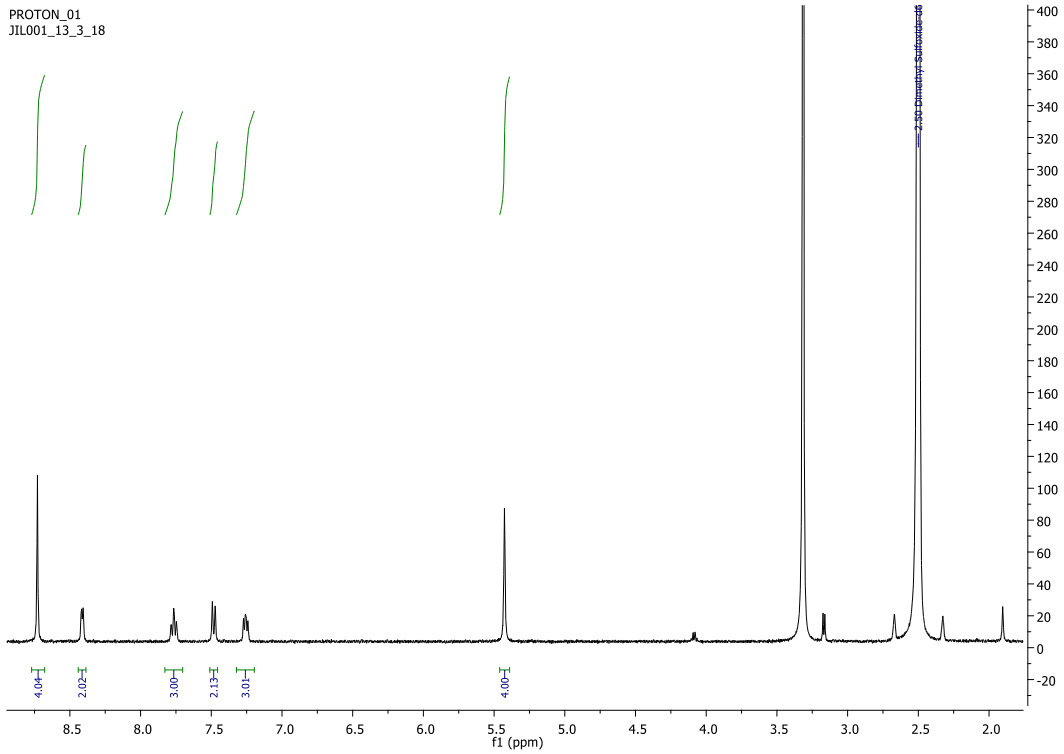


**Figure S20**: $^{1}$H spectra for **L1.**

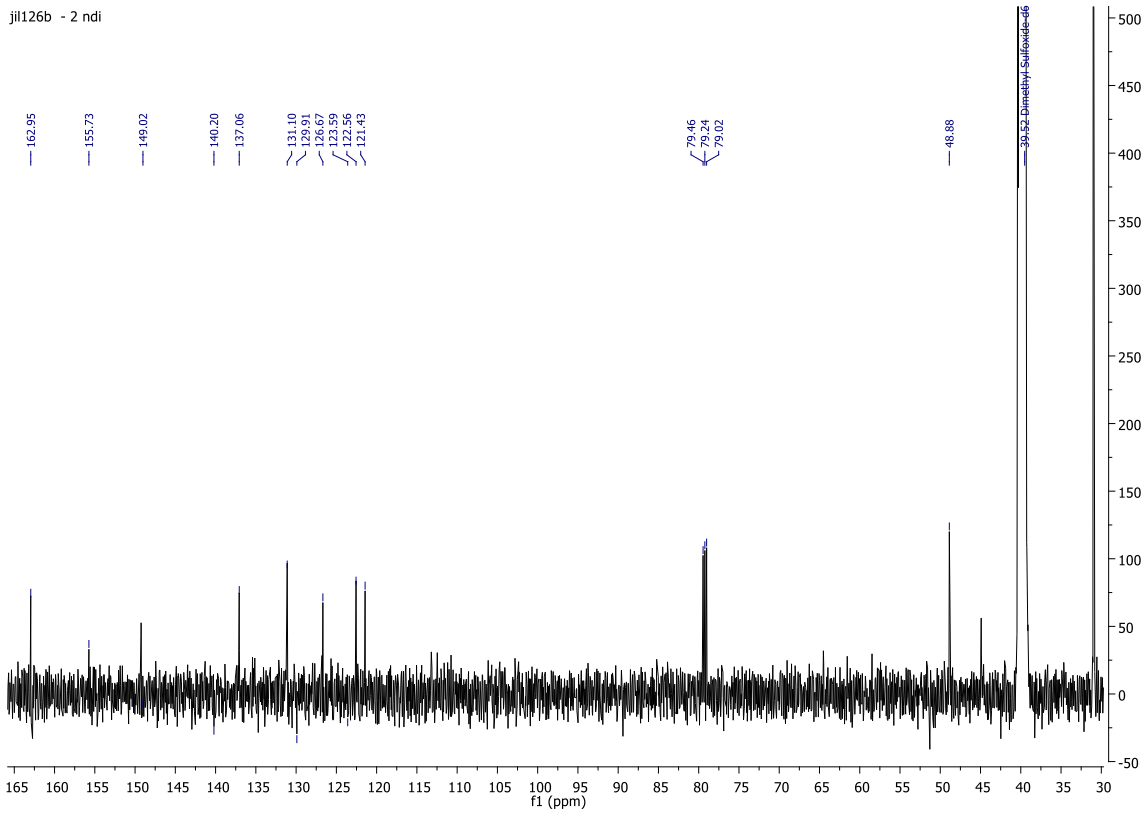


**Figure S21**: $^{13}$C spectra for **L1.**

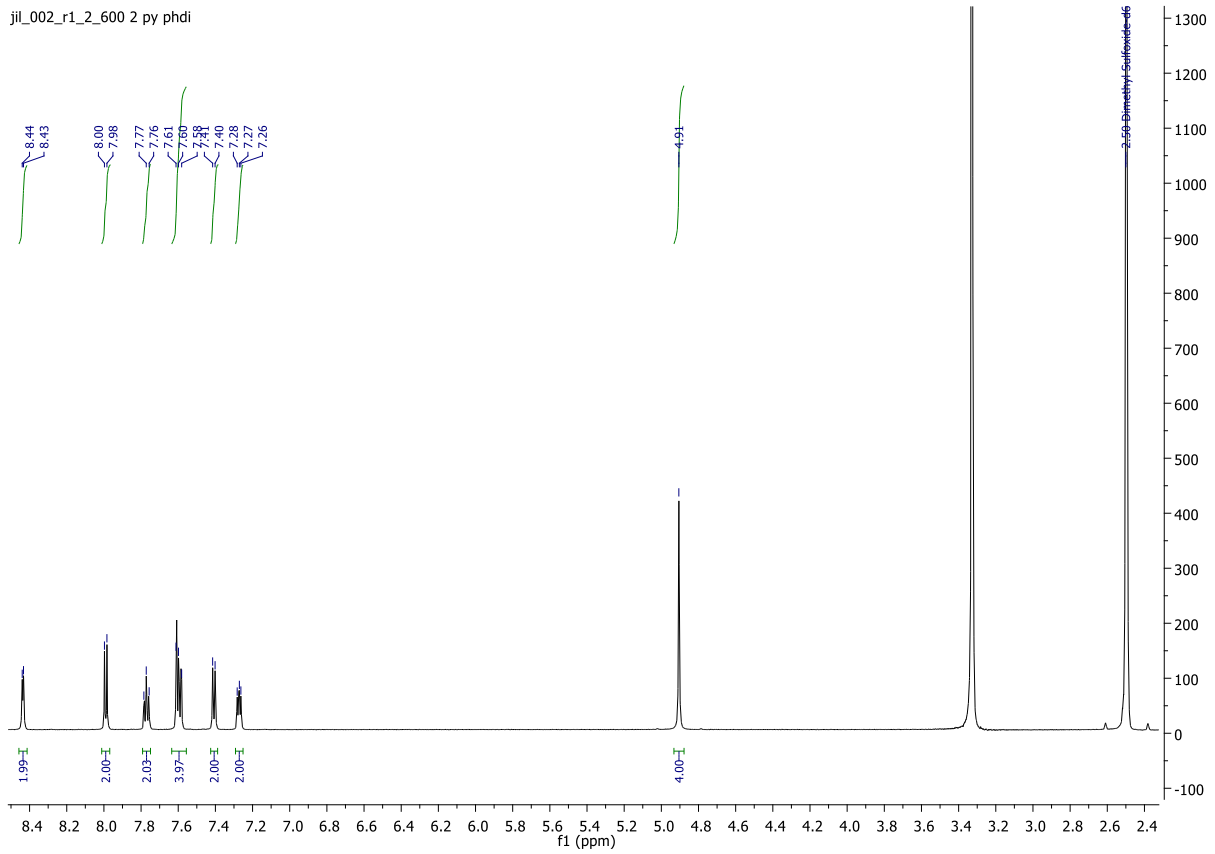


**Figure S22**: $^{1}$H NMR spectra for **L2.**

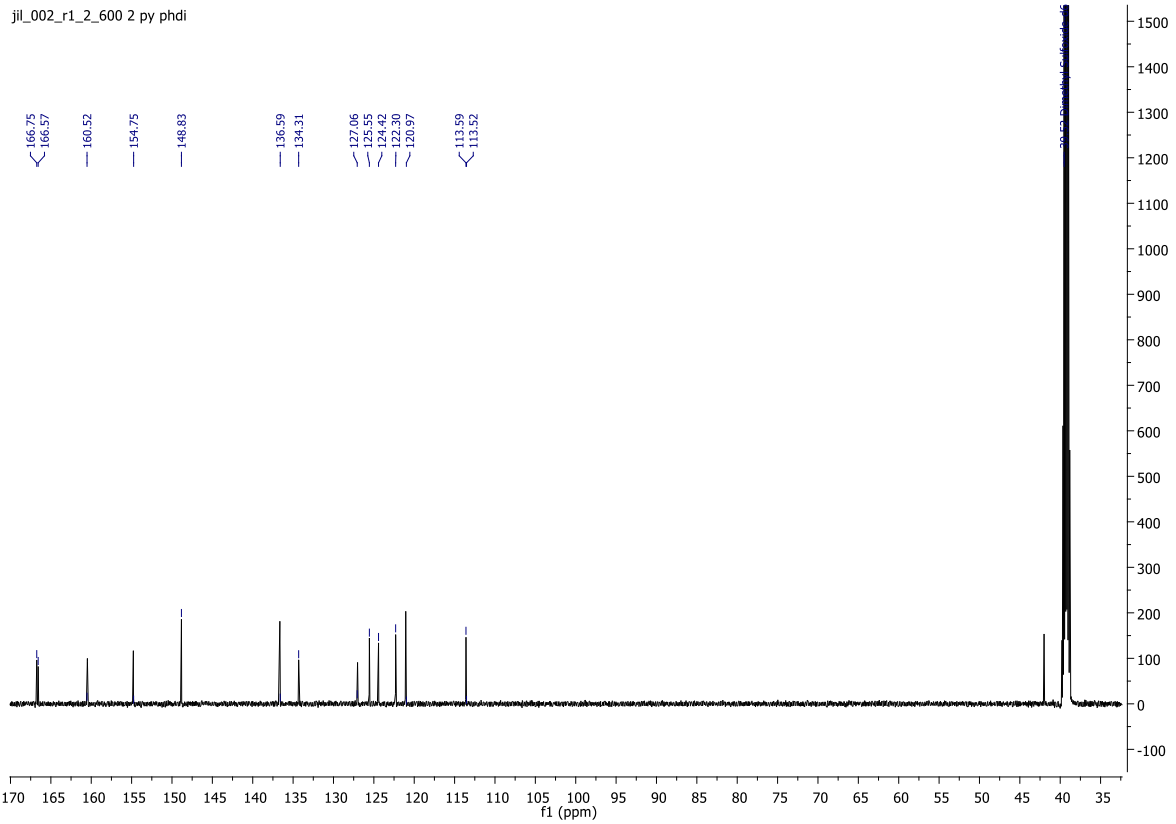


**Figure S23**: $^{13}$C NMR for **L2.**

## 5. Hydrogen Bonding Parameters, Additional Crystallographic Figures, and Ellipsoid Plots

**Table S1:** Geometrical Parameters for classical hydrogen bonds in compounds 3 and 4

| **Compound** | D | H | A | d(D-H) (Å) | D(H-A) (Å) | D(D-A) (Å) | <DHA (°) |
|---|---|---|---|---|---|---|---|
| **3** | N1 | H1 | O5 | 0.88 | 2.06 | 2.940(5) | 177 |
| | N4 | H4 | O5 | 0.88 | 2.13 | 2.982(4) | 161.4 |
| | O7 | H7A | Cl3 | 0.87 | 2.19 | 3.030(7) | 163.1 |
| | O5 | H5A | Cl2 | 0.87 | 2.41 | 3.170(3) | 146.4 |
| | O6 | H6D | O5 | 0.87 | 2.28 | 3.033(7) | 144.3 |
| | | | | | | | |
| **4** | N1 | H1 | Cl1 | 1.15(9) | 1.86(9) | 2.993(9) | 166(7) |

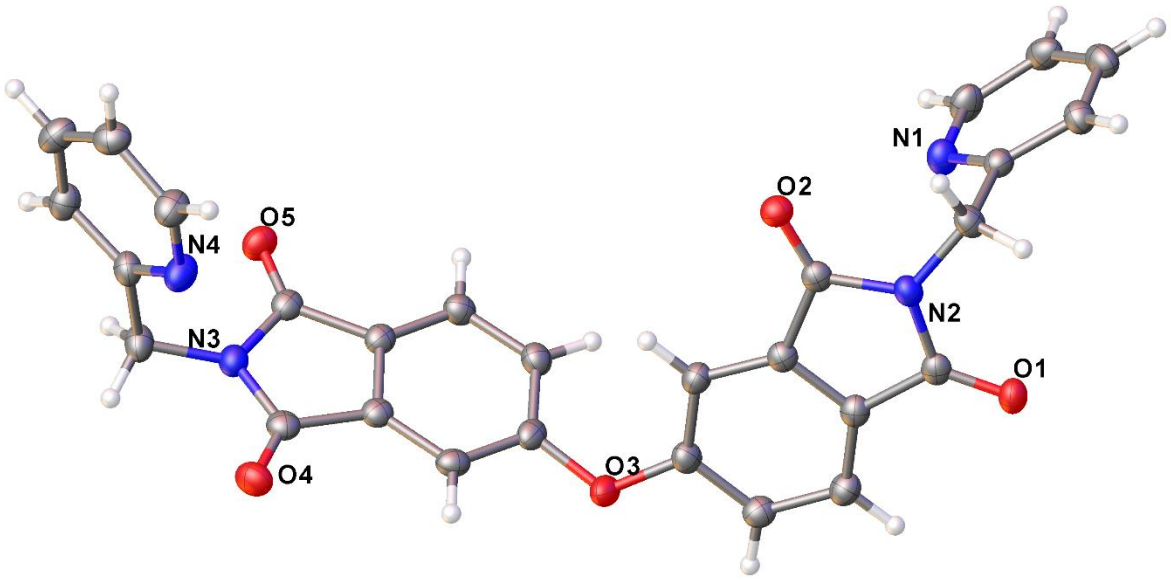


**Figure S24** Ellipsoid plot for the asymmetric unit of compound **L2** with heteroatom labelling scheme. Ellipsoids rendered at 50% probability level.

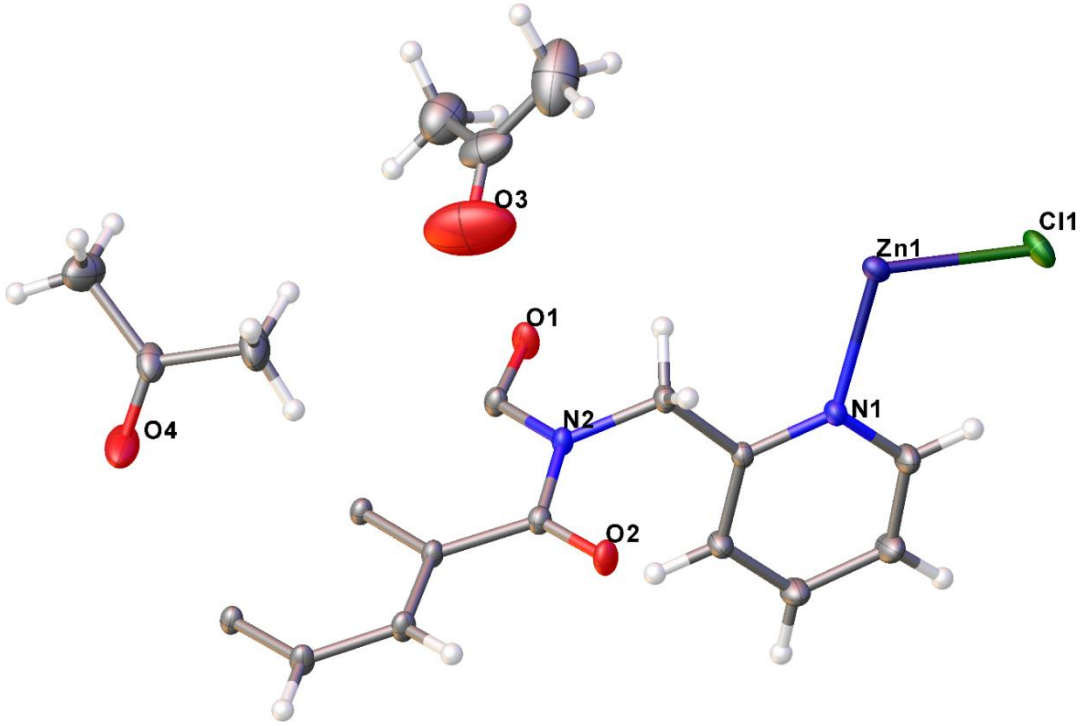


**Figure S25** Ellipsoid plot for the asymmetric unit of compound **1** with heteroatom labelling scheme. Ellipsoids rendered at 50% probability level.

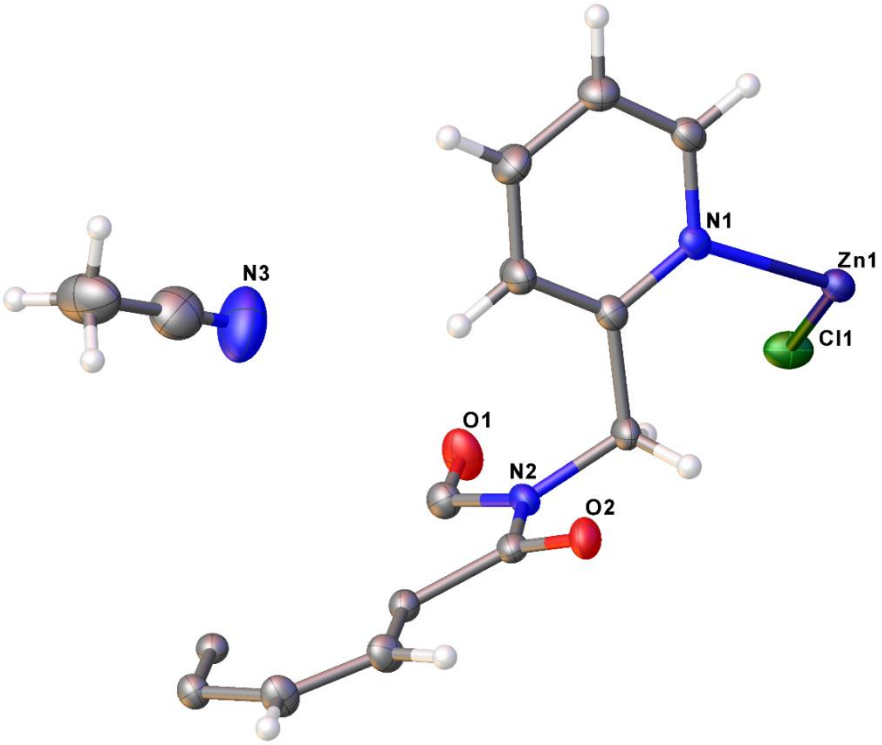


**Figure S26** Ellipsoid plot for the asymmetric unit of compound **2** with heteroatom labelling scheme. Ellipsoids rendered at 50% probability level.

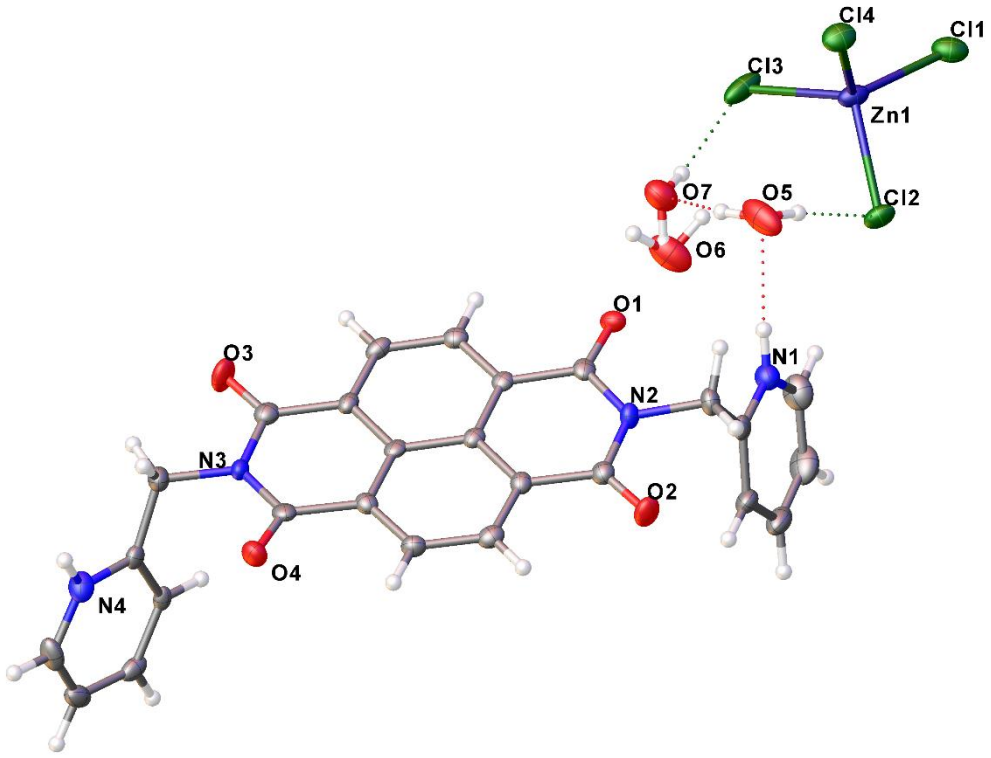


**Figure S27** Ellipsoid plot for the asymmetric unit of compound **3** with heteroatom labelling scheme. Ellipsoids rendered at 50% probability level.

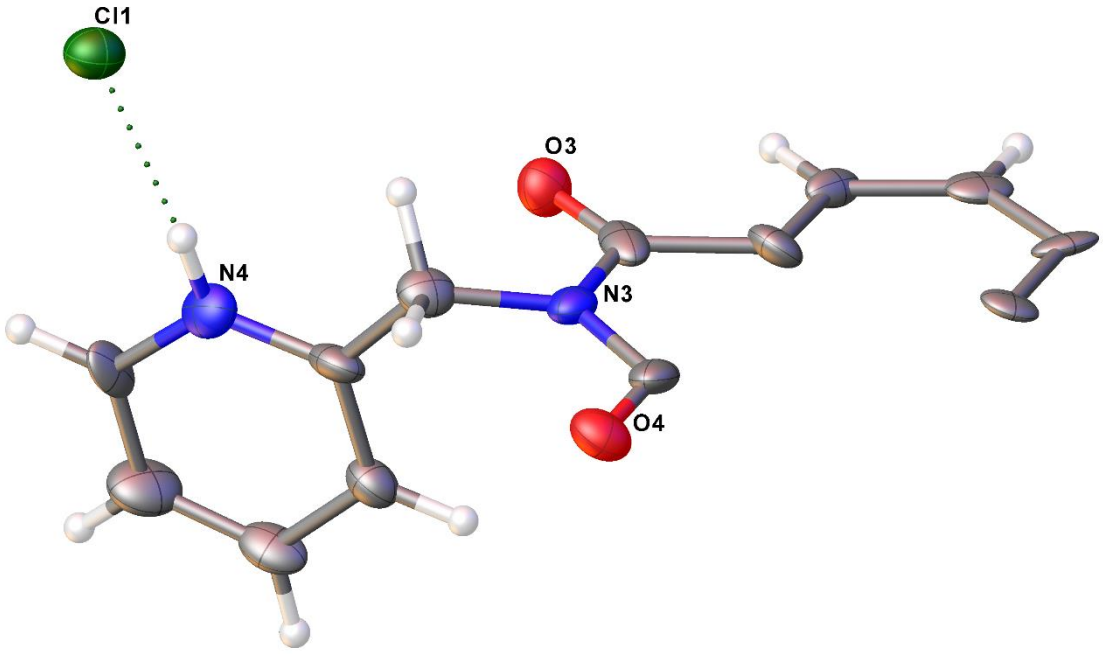


**Figure S28** Ellipsoid plot for the asymmetric unit of compound **4** with heteroatom labelling scheme. Ellipsoids rendered at 50% probability level.

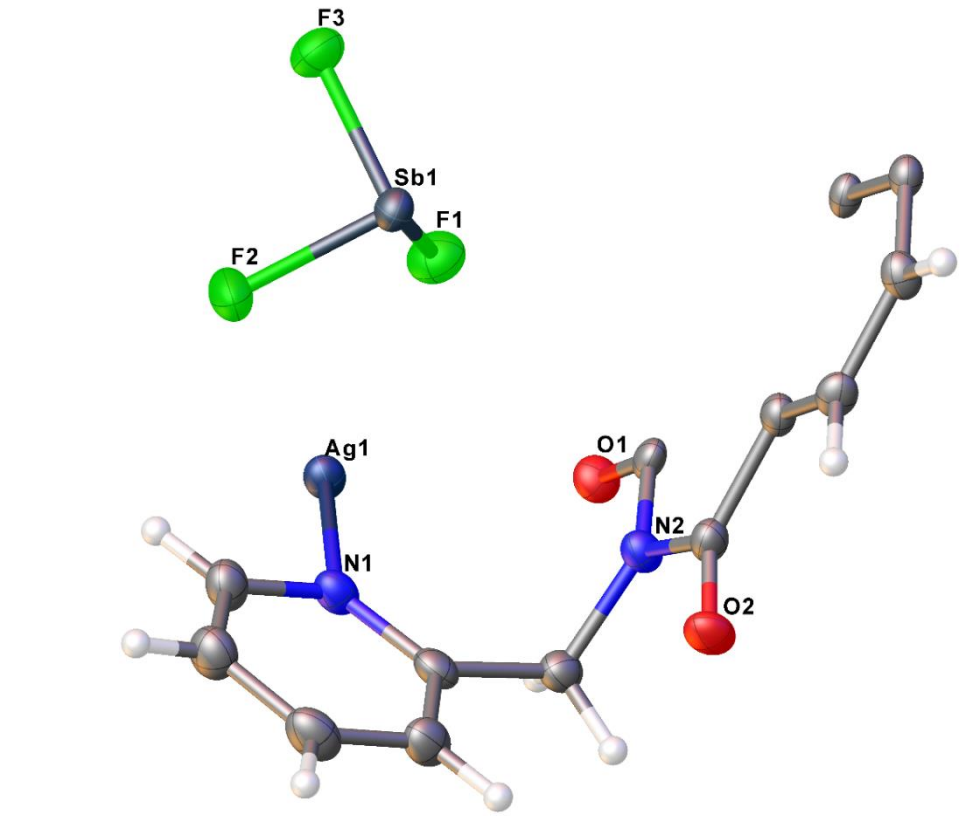


**Figure S29** Ellipsoid plot for the asymmetric unit of compound **5** with heteroatom labelling scheme. Ellipsoids rendered at 50% probability level.

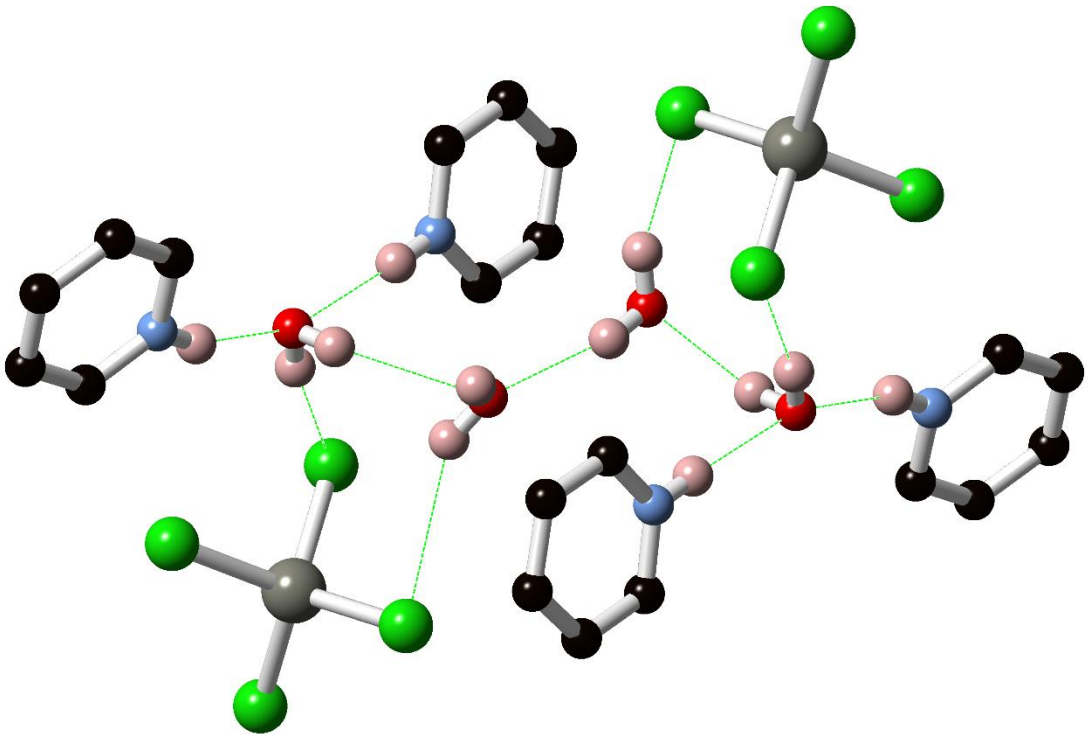

**Figure S30** Hydrogen bonding interactions in the structure of **3**, showing the predominant interaction modes involving the lattice water molecules, tetrachlorozincate and pyridinium groups (ligand backbone omitted). Major disordered contributors for lattice water molecules are shown only.